# Cyclohexylpiperazine derivative PB28, a $\sigma_2$ agonist and $\sigma_1$ antagonist receptor, inhibits cell growth, modulates P-glycoprotein, and synergizes with anthracyclines in breast cancer

Amalia Azzariti,[1] Nicola A. Colabufo,[2]
Francesco Berardi,[2] Letizia Porcelli,[1] Mauro Niso,[2]
Grazia M. Simone,[1] Roberto Perrone,[2]
and Angelo Paradiso[1]

[1]Clinical Experimental Oncology Laboratory, National Cancer
Institute; and [2]Dipartimento Farmaco-Chimico,
University of Bari, Bari, Italy

## Abstract

$\sigma$ Ligands have recently been shown to have cytotoxic activity, to induce ceramide-dependent/caspase-independent apoptosis, and to down-regulate P-glycoprotein (P-gp) mRNA levels in some mouse and human models. In this study, we verified whether a mixed $\sigma_2$ agonist/$\sigma_1$ antagonist, PB28, was able to have antitumor activity and to enhance anthracycline efficacy in two human breast cancer cell lines, MCF7 and MCF7 ADR, both characterized by significant $\sigma_2$ receptor expression, by high and low $\sigma_1$ receptor expression, and low and high P-gp expression, respectively. In both cell lines, PB28 showed high $\sigma_2$ receptor affinity and low $\sigma_1$ receptor affinity; furthermore, it inhibited cell growth with a clear effect at 48 hours (IC$_{50}$ in nanomolar range), a consistent time exposure-independent increase of G$_0$-G$_1$-phase fraction (of $\sim 20\%$ of both cell lines) and caspase-independent apoptosis (15% increased after 1-day drug exposure). PB28 also reduced P-gp expression in a concentration- and time-dependent manner ($\sim 60\%$ in MCF7 and 90% in MCF7 ADR). We showed also a strong synergism between PB28 and doxorubicin by adopting either simultaneous or sequential schedules of the two drugs. We suggest that this synergism could depend on PB28-induced increase of intracellular accumulation of doxorubicin ($\sim 50\%$ in MCF7 and 75% in MCF7 ADR by flow cytometry analysis). In conclusion, we suggest that the $\sigma_2$ agonist PB28 could be an interesting antitumor agent either in monotherapy or in combination with conventional drugs. [Mol Cancer Ther 2006;5(7):1807–16]

## Introduction

$\sigma$ Receptors have been described in human cells by Martin et al. (1) and classified into two distinct class, $\sigma_1$ and $\sigma_2$. These receptors have been recognized in the central nervous system, in endocrine tissues, in the liver and kidneys, and in immune system cells; now, most of their physiologic functions have been studied and elucidated (2–4). High levels of $\sigma_1$ receptors have also been found in embryonic stem cells (5). At subcellular level, $\sigma_1$ receptors seems to be localized in the plasma membrane, mitochondria, and endoplasmic reticulum (6–9). By contrast, the localization of $\sigma_2$ receptors is still unknown. The $\sigma_1$ receptor has been isolated and its cDNA has been cloned (10). The receptor protein (25 kDa) consists of 223 amino acids and displays 30% homology with the $\Delta_8$-$\Delta_7$ isomerase even if the $\sigma_1$ receptor has no enzyme activity. The characteristics of the $\sigma_2$ receptor are less known because of the lack of potent and selective ligands, which makes its purification and characterization very difficult (11). In the central nervous system, the $\sigma_1$ subtype is involved in the modulation of K$^+$ and Ca$^{2+}$ channels and in $N$-methyl-D-aspartate, serotonergic, dopaminergic, and muscarinic neurotransmission (12–14).

Both $\sigma$ receptor subtypes are expressed in human tumor cells; furthermore, recent experimental results have shown that the differential expression of each subtype could be of prognostic value (15–17). It has been also reported that $\sigma_2$ expression is related to tumor growth rate, supporting the idea that it could be a reliable tumor cell proliferation biomarker (18, 19). The high expression of $\sigma_2$ receptors by a variety of cancer cell lines has also suggested that they may be used as targets for antitumor agents. Preliminary studies have confirmed that $\sigma$ receptor ligands are able to kill glioma cells and the cytotoxic effects of these drugs have been found to be mediated specifically by the $\sigma_2$ receptor subtype (20–22). Pharmacologic studies have shown that $\sigma_2$ receptor agonists induce the modulation of different cell processes by promoting Ca$^{2+}$ depletion from endoplasmic and mitochondrial stores and inducing caspase-independent apoptosis (23–25). These compounds were also able to decrease P-glycoprotein (P-gp or MultiDrug Resistance-1; ref. 26), which is one of the three major groups of ATP-binding cassette transporters involved in multidrug resistance (MDR; ref. 27) together with other MRP proteins and ABCG2. Many cytotoxic drugs, such as anthracyclines (28),

taxanes (29), and camptothecins (30), are susceptible to MDR-mediated loss of sensitivity through P-gp and ABCG2, respectively. Actually, several strategies have been developed acting on MDR mostly through inhibition or modulation of P-gp (28) and several phase I and II trials with P-gp inhibitors are ongoing (31).[3]

Recently, we synthesized several ligands with high $\sigma_2$ receptor affinity and only moderate selectivity toward $\sigma_1$ receptors (32); among these ligands, the cyclohexylpiperazine derivative PB28 displayed $\sigma_2$ receptor agonist activity in an isolated guinea pig bladder bath (33) as well as antiproliferative and cytotoxic effects in both C6 rat glioma and SK-N-SH human neuroblastoma cell lines (34). There is evidence in the literature that other $\sigma_2$ agonists produce dose-dependent cytotoxicity in antineoplastic sensitive and resistant breast cancer cells (15). This finding lends credit to the hypothesis that PB28 could be a useful antitumoral agent as well as a drug resistance revertant.

This study characterized PB28 biological activity in two breast cancer cell lines that differed in terms of their anthracycline resistance characteristics and $\sigma$ receptor affinity by investigating its ability to inhibit cell growth, to induce apoptosis, to modify cell cycle distribution, and to decrease P-gp expression. The PB28-dependent modulation of intracellular doxorubicin accumulation as well as the possibility to enhance doxorubicin chemosensitivity by adopting different PB28 and anthracycline combination schedules was also evaluated.

## Materials and Methods

### Drugs and Chemicals

PB28 dihydrochloride was synthesized in our laboratories as described by Berardi et al. (35). Stock solutions were prepared at 1 mmol/L in absolute ethanol and stored in aliquots at 4°C. Doxorubicin was provided by Sigma-Aldrich (Milan, Italy) and dissolved at 20 mmol/L in DMSO, with aliquots kept at −20°C. Verapamil was provided by Tocris Life Sciences (Sussex, United Kingdom) and dissolved at 1 mmol/L in distilled water. Further dilutions were made in a medium supplemented with 10% fetal bovine serum (FBS), 2 mmol/L glutamine, 50,000 units/L penicillin, and 80 μmol/L streptomycin. [3H]DTG and (+)-[3H]pentazocine were purchased from Perkin-Elmer Life Sciences (Zavantem, Belgium). DTG was purchased from Tocris Cookson (Bristol, United Kingdom) and (+)-[3H]pentazocine was purchased from Sigma-Aldrich. 3-(4,5-Dimethylthiazol-2-yl)-2,5-diphenyltetrazolium bromide (MTT; Sigma, St. Louis, MO) was dissolved in PBS to a concentration of 5 mg/mL.

### Cell Lines

The two breast cancer cell lines of human origin, MCF7 and MCF7 ADR (resistant to Adriamycin or doxorubicin), were kindly provided by Prof. G. Zupi (IRE, Rome, Italy) and the colon cancer cell line HCT-15 was obtained by the National Cancer Institute (Frederick, MD). The cells were routinely cultured in RPMI 1640 supplemented with 10% FBS, 2 mmol/L glutamine, 50,000 units/L penicillin, and 80 μmol/L streptomycin in a humidified incubator at 37°C with a 5% $CO_2$ atmosphere. The cells were trypsinized once or twice weekly with trypsin/EDTA (0.25%/0.02%) and the medium was changed twice weekly. Doubling times were 48 ± 1 hours for MCF7 and 24 ± 1 hours for MCF7 ADR and HCT-15.

### Saturation and Competition Binding Assays

**Membrane Preparations.** The membrane preparations from the cell lines used in the saturation and competition binding assays were carried out as described elsewhere (33) with minor modifications. The cells were suspended in ice-cold buffer (20 mL) containing 0.32 mol/L sucrose and 10 mmol/L Tris (pH 7.4) and homogenized with a Potter-Elvehjem homogenizer (Teflon pestle). The homogenate was centrifuged at 4°C at 31,000 × $g$ for 15 minutes. The supernatant was discarded and the pellet was resuspended in 10 mmol/L Tris-HCl (pH 7.4) and stored at −80°C until use. For each membrane preparation, the protein content was determined by the Lowry method.

**Saturation Binding Assays.** The saturation binding assays were carried out as described by Colabufo et al. (33) with minor modifications. The $\sigma_2$ receptors were radiolabeled using [3H]DTG and the $\sigma_1$ receptors were radiolabeled using (+)-[3H]pentazocine in concentrations ranging from 1.0 to 150 nmol/L. Samples in a final volume of 500 μL for $\sigma_2$ receptor saturation contained 400 μg membrane protein, radioligand, 10 μmol/L DTG to determine $\sigma_2$ nonspecific binding, and 200 nmol/L (+)-[3H]pentazocine to mask $\sigma_1$ receptors. Samples in a final volume of 500 μL for $\sigma_1$ receptors contained 400 μg membrane protein, radioligand, and 1 μmol/L (+)-[3H]pentazocine to determine $\sigma_1$ nonspecific binding. The samples for both experiments were equilibrated in a final volume of 500 μL of 50 mmol/L Tris (pH 8.0) for 120 minutes at 25°C. Incubations were stopped by addition of 5 mL ice-cold buffer [10 mmol/L Tris (pH 7.4)], and the suspension was filtered through GF/C presoaked in 0.5% poly(ethylenimine) for at least 30 minutes before use. The filters were washed twice with 5 mL ice-cold buffer.

**Binding Competition Assays.** In the $\sigma_2$ competition binding assay, the samples contained 400 μg protein, 5.0 nmol/L [3H]DTG, 200 nmol/L (+)-[3H]pentazocine to mask $\sigma_1$ receptors in a final volume of 500 μL, and different concentrations of PB28. The subsequent manipulations were as described above for the saturation experiment. Nonspecific binding was determined in the presence of 10 μmol/L DTG. Specific binding ranged from 80% to 90% of the total.

The samples for the $\sigma_1$ competition binding assay contained 400 μg protein, 6 nmol/L (+)-[3H]pentazocine, 1 μmol/L (+)-[3H]pentazocine to determine nonspecific binding, and different concentrations of PB28. The subsequent manipulations were as described above for the saturation experiment. Specific binding ranged from 80% to 90% of the total.

### Evaluation of Cell Growth

Determination of cell growth was done using the MTT assay. On day 1, 10,000 cells per well were plated in 96-well plates in a volume of 200 μL, and on day 2, the various drugs alone or in combination were added. Six control wells (untreated cells) and six wells for each drug were used in each experiment. In all experiments, the various drug solvents (ethanol and DMSO) were added in each control to evaluate a possible solvent cytotoxicity. After the desired incubation time with the drug, 0.5 mg/mL MTT was added to each well, and after 1-hour incubation at 37°C, the supernatant was removed. To solubilize the formazan crystals, 100 μL DMSO was added and the absorbance values at 570 and 630 nm were determined on the microplate reader SpectraCount (Packard, Meriden, CT).

**$IC_{50}$ Determination.** PB28 was used at 0.01, 0.1, 1, 10, and 100 nmol/L for 1 and 2 days and doxorubicin was used at 0.01, 0.1, 1, 10, and 100 μmol/L for 3 days. The results for each drug were analyzed with the CalcuSyn software (Biosoft, Cambridge, United Kingdom) and the $IC_{50}$ was defined as the drug concentration yielding a fraction of affected (nonsurviving) cells equal to 50% compared with untreated controls. Each experiment was done in triplicate.

**Cell Viability after PB28 Exposure.** MCF7 and MCF7 ADR cells were incubated with PB28 at each $IC_{50}$ concentration for 2 days; 10,000 cells per well of drug-treated and untreated cells (control) were plated in 96-well plates, and after 3 days, the cell growth was measured using the MTT assay. The drug reduction of cell viability was measured as the percentage of cell growth decrease as respect to the control.

**Effect of Antiproliferative Drug Combination.** In MCF7 and MCF7 ADR, PB28 was used at each $IC_{50}$ concentration for 2 days and doxorubicin was used at 1, 5, 10, 50, and 100 μmol/L for 3 days. The two schedules used were (*a*) simultaneous (i.e., PB28 and doxorubicin were added simultaneously for 2 days, and after two wash steps, doxorubicin was administered for an additional day) and (*b*) sequential (i.e., PB28 was administered for 2 days, and after two wash steps, doxorubicin was administered for 3 days). Each experiment was done in triplicate. The results were analyzed with the CalcuSyn software to determine dose-response interactions (antagonism, additivity, and synergism) expressed as a nonexclusive case combination index (CI) for every fraction affected (36). Drug combinations were classified as very strong synergistic for CIs < 0.1, strong synergistic for CIs between 0.1 and 0.3, and synergistic for CIs between 0.3 and 0.7.

The experiments of MCF7 and MCF7 ADR cells exposed to the P-gp inhibitor verapamil were carried out using the following sequence: PB28 at $IC_{50}$ concentration of each cell line for 2 days followed by verapamil at 20 μmol/L for 2 hours and then doxorubicin at 5 μmol/L for 3 days. Briefly, verapamil is considered a P-gp competitive inhibitor with a double activity; at high concentrations, it inhibits P-gp activity conversely, and at low concentrations, it is a P-gp substrate (37). In *in vitro* studies concerning its ability as inhibitor, verapamil is used in a micromolar range (38).

In the kinetic experiments and in both cell lines, doxorubicin was used at 5 μmol/L, corresponding to the $IC_{50}$ concentration in MCF7 cells, because verapamil should restore doxorubicin effectiveness in MCF7 ADR. Cell growth inhibition by drugs exposure was analyzed with respect to the cell growth of drug-untreated cells.

### P-gp, Epidermal Growth Factor Receptor, ABCG2, Akt, and Erk1/2 Analysis

MCF7 and MCF7 ADR cells were exposed to 50 and 100 nmol/L PB28 and to their corresponding $IC_{50}$ concentration (25 and 15 nmol/L, respectively) for 1 and 2 days. In all experiments, ethanol was added in each control to evaluate the possible cytotoxicity of the solvent. To analyze the recovery of protein expression levels, cells were exposed to PB28 for 2 days with 1 day of drug washout. P-gp level was measured by Western blotting and flow cytometry.

**Western Blot.** Proteins were extracted from $3 \times 10^6$ cells by homogenization in radioimmunoprecipitation assay buffer [0.5 mol/L NaCl, 1% Triton X-100, 0.5% NP40, 1% deoxycholic acid, 3.5 mmol/L SDS, 8.3 mmol/L Tris-HCl (pH 7.4), 1.6 mmol/L Tris] and treated with 20% protease inhibitor cocktail (Sigma). Total proteins were measured by the Bradford method and 25 to 50 μg were electrophoretically separated on 10% to 12.5% acrylamide gel (SDS-PAGE by Laemmli). The monoclonal anti-P-gp (MDR) clone F4 was from Sigma, anti–epidermal growth factor receptor (clone 13) was from BD Transduction Laboratories (San Diego, CA), anti-Akt and anti-Erk1/2 were from Cell Signaling Technology (Beverly, MA), and anti-ABCG2 (clone BXP-21) was from Alexis Corp. (Lausen, Switzerland).

The signal was detected by chemiluminescence assay (Enhanced Chemiluminescence Plus, Amersham Life Science, Buckinghamshire, United Kingdom). The expression level was evaluated by densitometric analysis using Quantity One software (Bio-Rad, Hercules, CA) and β-actin (Sigma) expression level was used to normalize the sample values.

**Flow Cytometry.** Untreated and PB28-treated cells were harvested, washed twice in ice-cold PBS (pH 7.4), fixed in 4.5 mL of 70% ethanol, and stored at −20°C. Fixed cells were washed in ice-cold PBS once and incubated in 0.5 mL of 0.1% Tween 20 in PBS for 15 minutes at 25°C. To analyze P-gp expression after drug exposure, untreated (control) and PB28-treated cells (samples) were incubated overnight at 4°C with a monoclonal anti-P-gp (MDR) clone F4 (Sigma; 1:25 dilution) in 0.5% Tween 20 and 1% FBS in PBS; to determine the unspecific fluorescence due to the fluorescein-conjugated secondary antibody, untreated cells were incubated with an appropriate isotype control (50 μg/$10^6$ cells) in the same experimental conditions (isotype control). After 15-minute incubation with 0.5 mL of 0.5% FBS in PBS, cells were centrifuged and washed once in 0.5 mL of 0.5% FBS in PBS. The pellet was resuspended in 0.5% FBS in PBS in the presence of the goat anti-mouse IgG (H&L) fluorescein-conjugated affinity-purified secondary antibody (Chemicon International, Temecula, CA; 1:50) and incubated for 1 hour at 4°C. After a wash step with 0.5 mL

of 0.5% FBS in PBS, cells were centrifuged and incubated in 5 µg/mL propidium iodide overnight at 4°C. P-gp protein determination was done using a FACScan flow cytometer (Becton Dickinson, NJ). Fluorescence analysis was gated to include single cells based on forward and side light scatter and was based on the acquisition of data from 10,000 cells. Log fluorescence was collected and displayed as single-variable histograms. The data analysis was carried out with the CellQuest software (Becton Dickinson). Relative fluorescence (% P-gp reduction) represented a ratio obtained through the following formula:

$$\%P - gp = \frac{(FM_S - FM_{IC})}{(FM_C - FM_{IC})} \times 100,$$

where $FM_S$ is mean fluorescence of the PB28-treated sample, $FM_{IC}$ is mean fluorescence of the isotype control, and $FM_C$ is mean fluorescence of the control.

### Cell Cycle Perturbation

MCF7 and MCF7 ADR cells were exposed to PB28 at 25 and 15 nmol/L, respectively, for 1 to 2 days. In all experiments, ethanol was added in each control to evaluate the solvent influence. Cells were harvested, washed twice in ice-cold PBS (pH 7.4), fixed in 4.5 mL of 70% ethanol at −20°C, and then washed once in ice-cold PBS. The pellet was resuspended in PBS containing 1 mg/mL RNase and 0.01% NP40, and cellular DNA was stained with 50 µg/mL propidium iodide (Sigma). Cells were stored in ice for 1 hour before analysis. Cell cycle determinations were done using a FACScan flow cytometer, and percentages of each cell cycle phase ($G_0$-$G_1$, S, and $G_2$-M) were obtained using the ModFit software provided by the manufacturer.

### Analysis of Apoptosis and Caspase Activation

**Apoptosis Determination.** Apoptosis detection was done by Annexin V-FITC staining assays (Biovision, Palo Alto, CA). Five million cells exposed to PB28 or with the solvent ethanol were incubated with Annexin V at room temperature for 10 minutes following the manufacturer's instructions. Apoptotic cells were detected by fluorescence-activated cell sorting analysis (Becton Dickinson) quantified using the CellQuest software and expressed as percentage of apoptotic cells.

**Caspase-3/7 Assay.** Caspase activation was done by Apo-One Homogenous Caspase-3/7 kit (Promega Corp, Madison, WI) and measured as the amount of fluorescent product generated from the cleavage of a profluorescent substrate Z-DEVD-R110. Cells were seeded into 96-well plates for optical performance in the fluorescent cell-based assay in 100 µL complete medium in the presence or absence of different concentrations of PB28 using 0.1 µmol/L staurosporine as positive control for caspase-3/7-dependent apoptosis (39). The plate was incubated for 24 hours in a humidified 5% $CO_2$ atmosphere at 37°C and 100 µL substrate buffer mix was added. Plates were kept protected from light for 18 hours at room temperature and fluorescence was then recorded with a 499 nm excitation wavelength and 521 nm emission wavelength in a Perkin-Elmer LS55 Luminescence Spectrometer.

### Intracellular Doxorubicin Accumulation

The time course of doxorubicin intracellular accumulation and its modulation by PB28 were evaluated by flow cytometry. In all experiments, the various drug solvents (ethanol and DMSO) were added in each control to evaluate the solvent influence. In MCF7 and MCF7 ADR, doxorubicin and PB28 were used at each $IC_{50}$ concentrations for various time exposures using the same schedules as for the study of cytotoxicity. After incubation, the cell medium was removed and trypsin/EDTA was used to detach the cells from the plates. Cells were harvested, washed twice in ice-cold PBS (pH 7.4), and placed on ice (<1 hour) until analysis. Fluorescence measurements of individual cells were done with a Becton Dickinson FACScan equipped with an UV argon laser. Analysis was gated to include single cells based on forward and side light scatter and was based on the acquisition of data from 10,000 cells. Log fluorescence was collected and displayed as single-variable histograms. The mean fluorescence intensity of doxorubicin in the doxorubicin-treated cells, arbitrarily established as 100%, represented the positive control ($MF_{PC}$). The autofluorescence of untreated cells, arbitrarily established as 0%, was the negative control ($MF_{NC}$). The doxorubicin mean fluorescence intensity of doxorubicin in the PB28 plus doxorubicin-treated cells was $MF_S$. The amount of doxorubicin in the samples was obtained by the following formula:

$$\% \text{ Doxorubicin in samples} = \frac{MF_S - MF_{NC}}{MF_{PC} - MF_{NC}} \times 100$$
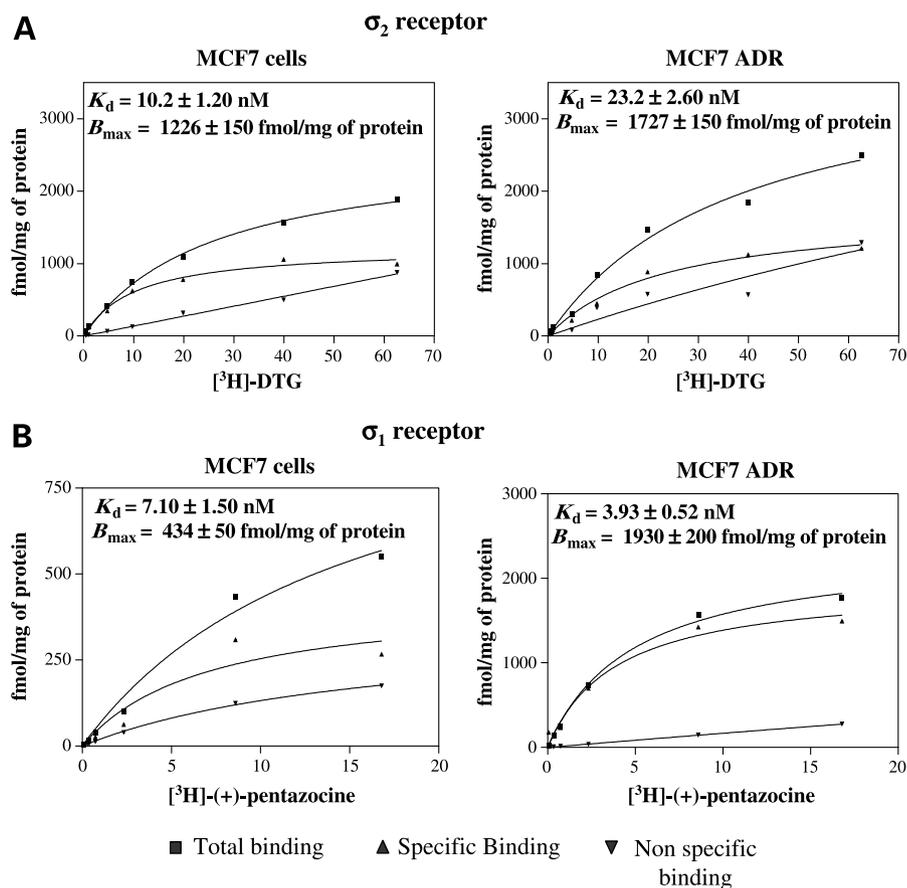
### Biostatistical Analysis

All of the *in vitro* experiments were done in triplicate and shown as mean ± SD unless otherwise indicated. Pearson's coefficient was used for correlation analysis. Saturation results, $K_d$ (radioligand concentration binding 50% of total σ receptors in the steady state) and $B_{max}$ (a value quantifying σ receptors in a biological sample), were analyzed by nonlinear curve fitting using the GraphPad Prism program (GraphPad Software, Inc., San Diego, CA). The $K_i$s (the drug concentration inhibiting 50% of radioligand binding to the σ receptors) were determined by a subsequent conversion of $IC_{50}$ to $K_i$s using the Cheng and Prusoff equation (40). Values are mean ± SE from three experiments in triplicate.

## Results

### Characteristics of σ₁ and σ₂ Receptors and PB28 Affinity

The expression of σ receptors in MCF7 and MCF7 ADR cells was shown by radioligand saturation analysis (Fig. 1). High σ₂ expression expressed as $B_{max}$s was found in both cell lines (1,226 fmol/mg protein in MCF7 cells and 1,727 fmol/mg protein in MCF7 ADR cells) with only slight differences in the $K_d$s of [³H]DTG (10.2 nmol/L in MCF7 cells and 23.2 nmol/L in MCF7 ADR cells). Conversely, the characteristics of the two cell lines were different for the σ₁

**Figure 1.** Saturation analysis of $\sigma_2$ and $\sigma_1$ receptors. Curves of saturation analysis of $\sigma_2$ (**A**) and $\sigma_1$ (**B**) receptor membrane preparations from MCF7 and MCF7 ADR cell lines. *Points,* mean of three independent experiments (samples in triplicate); *bars,* SE.



**A**    $\sigma_2$ receptor

**MCF7 cells**

$K_d = 10.2 \pm 1.20$ nM
$B_{max} = 1226 \pm 150$ fmol/mg of protein

[³H]-DTG

**MCF7 ADR**

$K_d = 23.2 \pm 2.60$ nM
$B_{max} = 1727 \pm 150$ fmol/mg of protein

[³H]-DTG

**B**    $\sigma_1$ receptor

**MCF7 cells**

$K_d = 7.10 \pm 1.50$ nM
$B_{max} = 434 \pm 50$ fmol/mg of protein

[³H]-(+)-pentazocine

**MCF7 ADR**

$K_d = 3.93 \pm 0.52$ nM
$B_{max} = 1930 \pm 200$ fmol/mg of protein

[³H]-(+)-pentazocine

■ Total binding    ▲ Specific Binding    ▼ Non specific binding

receptor. The MCF7 cells showed about four times less expression than did the MCF7 ADR cells ($B_{max} = 434$ fmol/mg protein, $K_d = 7.10$ nmol/L and $B_{max} = 1,930$ fmol/mg protein; $K_d = 3.93$ nmol/L, respectively).

After confirmation of the presence and function of the $\sigma$ receptors, we verified the affinity of our $\sigma_2$ receptor agonist, PB28, for both $\sigma$ receptors by competition binding assays. Our drug had a higher $\sigma_2$ receptor affinity expressed as $K_i$ (0.28 and 0.17 nmol/L in MCF7 and MCF7 ADR cells, respectively) than $\sigma_1$ receptor affinity (13.0 and 10.0 nmol/L, respectively; Fig. 1).

This preliminary characterization showed that $\sigma$ receptors were present in both cell lines and that PB28 had a higher and specific affinity for the $\sigma_2$ isoform, thereby confirming the efficiency of our *in vitro* model to address the other issues we had planned to explore in our experiment.

### PB28 Antitumor Activity

In our breast cancer model, the efficacy of PB28 as an antitumor agent was evaluated by analyzing cell response to various drug concentrations and drug-time exposures. The two cell lines were investigated under the same experimental conditions to limit biological variability.

**Cell Growth Inhibition and Cell Cycle Modulation.** PB28-dependent cell growth inhibition in MCF7 and MCF7

ADR cells was evaluated by MTT assay using increased drug concentrations with 1 and 2 days of drug exposure. One-day PB28 exposure induced a very slight cell growth inhibition ($IC_{50}$ higher than 100 nmol/L in both cell lines), whereas a 2-day drug exposure showed $IC_{50}$s in the nanomolar range (Table 1). Cell viability after PB28 exposure in MCF7 and MCF7 ADR cells was investigated as described in Materials and Methods. Our results showed that, after PB28 washout, most part of still viable cells recovered the ability to grow (surviving fraction >90% in both cell lines).

The analysis of cell cycle effects of PB28 by flow cytometry showed an accumulation in the $G_0$-$G_1$ phase for both cell lines that were time and concentration independent; in fact, 1 to 2 days of drug exposure showed an increase in percentage of cells in $G_0$-$G_1$ cell cycle phase from $56 \pm 3\%$ to $71 \pm 3\%$ and from $57 \pm 2\%$ to $79 \pm 3\%$ of PB28-treated MCF7 and MCF7 ADR cells, respectively. Increasing concentrations of PB28 ranging from $IC_{50}$ (15 nmol/L in MCF7 ADR and 25 nmol/L in MCF7) to 100 nmol/L did not increase further this cell cycle phase accumulation.

**Apoptosis Induction and Caspase Activation.** The ability of 1-day PB28 exposure at different concentrations to induce early apoptosis was evaluated by Annexin V-flow cytometry analysis (41). In both cell lines, this phenomenon

**Table 1. PB28 affinity and activity evaluation in membrane preparations and in living cell lines**

| Cell line | Ki ± SE (nmol/L)* | | IC$_{50}$ ± SE (nmol/L)* | |
|---|---|---|---|---|
| | $\sigma_2$ | $\sigma_1$ | Exposure time | |
| | | | 1 d | 2 d |
| MCF7 | 0.28 ± 0.01 | 13.0 ± 2.5 | >>100 | 25 ± 1.3 |
| MCF7 ADR | 0.17 ± 0.05 | 10.0 ± 0.80 | >>100 | 15 ± 0.9 |

*Mean ± SE of three independent experiments.

was evident with a maximum increase in the fraction of Annexin V–positive cells from ∼3% to 15%. Variations of PB28 concentrations from IC$_{50}$ to 100 nmol/L did not change this percentage significantly (data not shown).

To investigate whether PB28-induced apoptosis was caspase dependent, the activation of caspase-3 and caspase-7 in cells, after PB28 exposure, was evaluated by a fluorescent assay. The fluorescent light values obtained were not statistically different [25 ± 3 and 20 ± 2 fluorescent light from PB28-treated cells and drug-untreated cells (control), respectively]; these data are consistent with a no caspase activation and suggest that our $\sigma_2$ agonist induces apoptosis not caspase dependent (23).

We concluded that PB28 is able to inhibit cell growth probably through an increase in G$_0$-G$_1$ cell cycle phase accumulation and to induce apoptosis through a caspase-independent pathway.

### PB28-Dependent Modulation of P-gp and Cytotoxic Activity of Doxorubicin

Based on preliminary evidence suggesting a role for the $\sigma_2$ agonist in modulating the expression of some drug resistance-associated proteins (26), we further investigated whether PB28 was effective in reducing the expression of the P-gp protein reported as involved in anthracycline resistance modulation (27, 28).

**Modulation of P-gp Expression.** Due to the low basal levels of P-gp in MCF7 cells (42, 43), we analyzed the ability of PB28 to modulate P-gp expression by either Western blotting or flow cytometry assays. With the analysis of P-gp expression in MCF7 ADR cells by Western blotting (data not shown) and flow cytometry highly correlated (>0.90 by Pearson's test), only the flow cytometry data were retained for further considerations. PB28 exposure decreased the expression of the drug efflux pump in a time- and concentration-dependent manner in both cell lines (Table 2); however, these effects were quantitatively more evident in MCF7 ADR cells where escalating drug concentrations (15–100 nmol/L) produced a reduction from ∼50% to 40% P-gp expression after 1 day of exposure and from ∼40% to 10% after 2 days (Fig. 2A and B). In PB28-treated MCF7 cells, the same effects ranged from 75% to 65% after 1 day of exposure and from 70% to 40% after 2 days (Table 2). Interestingly, drug removal induced a quite complete recovery of P-gp expression in 1 day (data not shown). Conversely, 2-day PB28 was shown not to

modulate the expression level of another ATP-binding cassette transporter, ABCG2, involved in resistance to topoisomerase I inhibitors (30) and of other proteins, such as epidermal growth factor receptor, Akt, and Erk1/2 (data not shown), suggesting a specific action on P-gp expression of this $\sigma_2$ agonist and not a generalized protein synthesis inhibition. Moreover, the specificity of the PB28-dependent inhibition of P-gp expression has been confirmed in a different tumor cell model, HCT-15, highly expressing P-gp protein (44). In HCT-15, we preliminarily determined the 2-day PB28 IC$_{50}$ concentration (10 µmol/L) and then measured the drug-dependent reduction of P-gp expression by flow cytometry, showing that PB28-treated HCT-15 had a reduced expression of this drug efflux pump of ∼50% with respect to the untreated cells.

**PB28-Dependent Enhancement of Doxorubicin Efficacy.** Moving from the hypothesis that PB28 in combination with other common antitumor agents could improve the cytotoxic activity of the latter, the *in vitro* cytotoxic effects of PB28 and doxorubicin combinations were assessed. In agreement with a previous *in vitro* study (45), a 10 times lower IC$_{50}$ of doxorubicin was observed in MCF7 than in MCF7 ADR (4.1 ± 0.8 and 62.6 ± 3.6 µmol/L, respectively). To evaluate whether the combined administration of PB28 (at IC$_{50}$ concentrations in MCF7 and MCF7 ADR for 2 days) and doxorubicin (1–100 µmol/L for 3 days) could improve the doxorubicin efficacy, two schedules of sequential (PB28 followed by doxorubicin) or simultaneous treatments were used. The combinations of PB28 and doxorubicin produced, at each drug concentration and in both cell lines, a substantial increase in cytotoxicity compared with doxorubicin alone (Fig. 3). The CI for the sequential and simultaneous schedules of PB28 plus doxorubicin showed a very strong synergism (CI = 0.089) and a strong synergism (CI = 0.189) in the MCF7 cells; in the MCF7 ADR cells, the same schedules resulted in a synergistic effect (CI = 0.624 and 0.688, respectively).

**Correlation between P-gp Inhibition and Increased Doxorubicin Activity.** The hypothesis of a direct relationship between the ability of PB28 to reduce P-gp expression

**Table 2. Modulation of P-gp expression level by flow cytometry**

| Time exposure | P-gp expression (%)* | | | |
|---|---|---|---|---|
| | MCF7 | | MCF7 ADR | |
| | 1 d | 2 d | 1 d | 2 d |
| Control | 100 | 100 | 100 | 100 |
| PBS (nmol/L) | | | | |
| 15 | | | 53 ± 3.5 | 39 ± 4 |
| 25 | 75 ± 3 | 70 ± 4 | | |
| 50 | 70 ± 5 | 53 ± 4.6 | 50 ± 2.6 | 24 ± 4.2 |
| 100 | 64 ± 3.4 | 41 ± 2.9 | 42 ± 2.8 | 12 ± 2.1 |

NOTE: Percent P-gp expression in cells treated with various concentration of PB28 in function of time exposure.
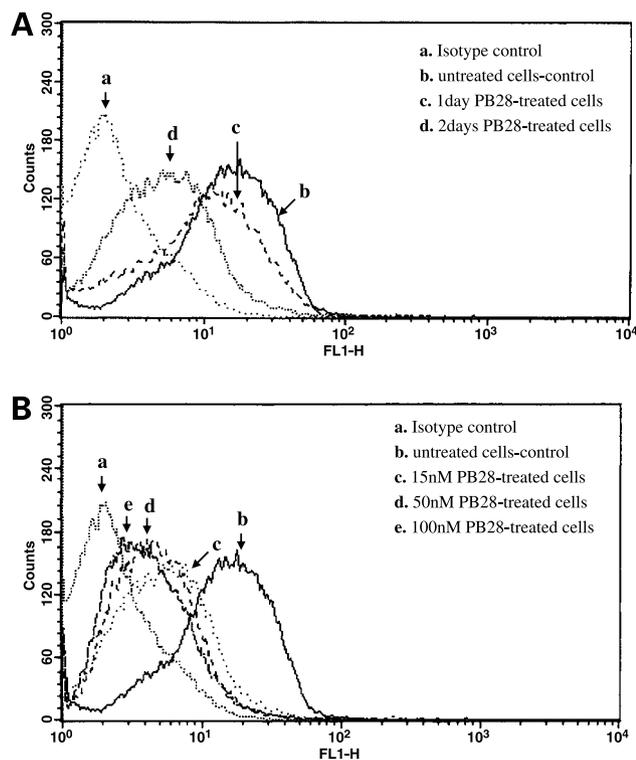*Mean ± SE of three independent experiments.

**Figure 2.** P-gp modulation in MCF7 ADR. Cells were incubated with PB28 at various concentrations and for various time exposures and the P-gp expression level was determined by flow cytometry as described in Materials and Methods. **A,** curves of P-gp after 1 and 2 d of PB28 ($IC_{50}$) exposure compared with baseline P-gp expression. **B,** concentration-dependent curves of P-gp modulation after 2 d of PB28 exposure compared with baseline P-gp expression.

level and the synergistic effect shown for its combination with doxorubicin was investigated by analyzing (*a*) the cytotoxicity of the combination in the presence or absence of the specific P-gp activity inhibitor verapamil and (*b*) the PB28-dependent modulation of intracellular doxorubicin accumulation.

As shown in Fig. 4, both cell lines resulted less sensitive to PB28-doxorubicin treatment in presence of verapamil than without, with respect to doxorubicin alone (from ∼30% to 10% of increased drug cytotoxicity in both cell lines).

Moreover, we analyzed the ability of PB28 to modulate intracellular doxorubicin accumulation through its possible role on the drug efflux pump P-gp. One day of doxorubicin exposure was enough to achieve a plateau accumulation in the cells (Fig. 5A). After having verified that PB28 had no autofluorescence characteristics, PB28-dependent modulation of doxorubicin accumulation was determined using the two schedules (sequential PB28 before doxorubicin or simultaneous) already described. In both cell lines, the sequential schedules induced a greater intracellular concentration of doxorubicin than the simultaneous one (Table 3). In Fig. 5B, we reported the results of these experiments in the MCF ADR cell line.

## Discussion

The study of new σ receptor ligands is of potential great interest for the development of new target-oriented strategies in cancer therapy. The biological bases of this study lie in the high density of σ receptors in tumor tissues compared with normal tissues (46), especially in breast cancer (16), and in the prolonged retention of σ receptor ligands in tumor cells compared with normal cells (47). There is evidence in the literature that σ receptor ligands (especially $\sigma_2$ selective agents) may represent lead radioimmunotherapeutics with $\sigma_2$ receptor-mediated cytotoxic effects (48). These compounds have been shown to produce dose-dependent cytotoxicity when used alone or in combination with DNA-damaging antineoplastic agents and to induce various cell effects, such as increased intracellular $Ca^{2+}$ levels, induction of p53 genotype/caspase-independent apoptosis, and reduction of P-gp expression (15, 26).

Based on these biological evidence, we decided to study in an *in vitro* breast cancer model the cytotoxic effects of PB28, a new compound with high $\sigma_2$ receptor affinity and only moderate selectivity toward $\sigma_1$ receptors (32); however, hypothesizing also a role for this drug in modulation of drug resistance (15, 27, 28), we chose the MCF7 and MCF7 ADR cell lines characterized by low and high P-gp expression levels, respectively, high $\sigma_2$ receptor expression, different $\sigma_1$ receptor expression, and different p53 genotypes (wild-type in MCF7 and mutated in exon 5 by a 21-bp deletion in MCF7 ADR ref. 15).
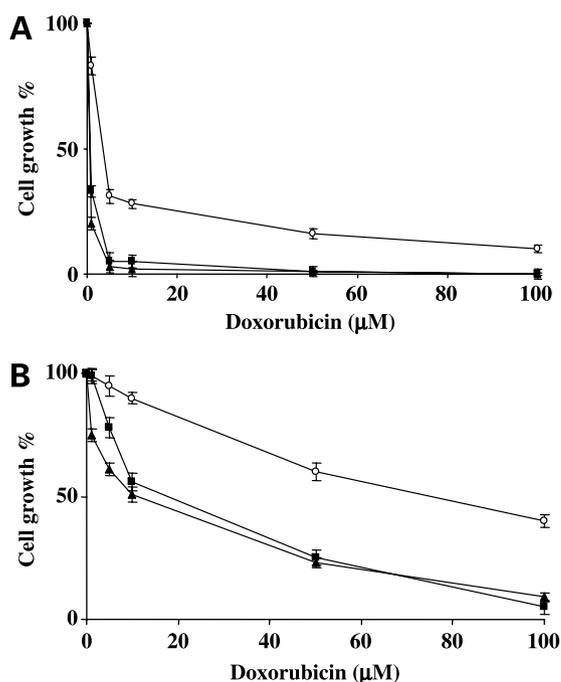


**Figure 3.** Cytotoxicity of doxorubicin in combination with PB28 in breast cancer model. Growth inhibition of MCF7 and MCF7 ADR cells after sequential (▲) or simultaneous (■) PB28 and doxorubicin administration compared with doxorubicin alone (○). **A,** plot of MCF7 growth inhibition (%) versus doxorubicin concentration (μmol/L). **B,** plot of MCF7 ADR growth inhibition (%) versus doxorubicin concentration (μmol/L).
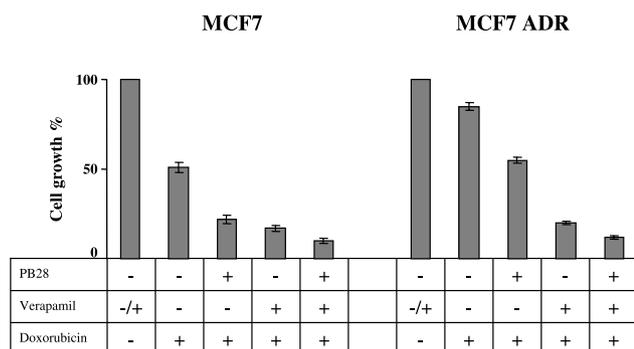
**Figure 4.** Cytotoxicity of PB28 plus doxorubicin in the presence or absence of verapamil. Percentage of MCF7 and MCF7 ADR cell growth inhibition after sequential PB28 and doxorubicin administration compared with doxorubicin in the presence or absence of verapamil.

In this model, we showed that PB28 inhibited cell growth, with an appreciable effect at 48 hours ($IC_{50}$ in nanomolar concentrations), and induced a caspase-independent apoptosis ($\sim 15\%$ of Annexin V–positive cells after 1-day PB28 exposure). These effects seem to stress the double nature of our $\sigma_2$ agonist PB28 showing both cytostatic and cytotoxic activities.

For what concerns the mechanisms of action, we showed in both cell lines that PB28 induced a time exposure-independent cell cycle block in the $G_0$-$G_1$ phase with an increase of $\sim 50\%$ of cells; interestingly, it was also able to reduce P-gp expression levels in a concentration-dependent and time exposure-dependent manner (inhibition from 25% to 60% in MCF7 cells and from 50% to 90% in MCF7 ADR cells). Finally, our analysis showed that PB28 capability to reduce P-gp expression was specific, not related to a generalized protein synthesis inhibition, and not tumor model dependent.

The absence of a correlation between the activity of $\sigma$ receptor ligands and p53 status, already reported by Crawford and Bowen (15), was confirmed by our results; in fact, the behavior of the two cell lines, MCF7 with p53 wild-type and MCF7 ADR p53 mutated, was similar after drug exposure. Moreover, we hypothesize that the consistent cell accumulation in $G_0$-$G_1$ phase after PB28 exposure could be responsible for the drug-dependent cell growth inhibition perhaps mediated by the down-modulation of voltage-operated $K^+$ channels that $\sigma_1$ receptors are able to regulate (49).

As suggested by other authors, PB28-dependent apoptosis is not characterized by caspase involvement, confirming that it could be mediated by the sphingolipid pathway through $Ca^{2+}$ signaling modulation. In fact, $\sigma_2$ agonists may increase ceramide levels and decrease sphingomyelin (23).

In summary, all these findings confirmed the ability of PB28 to decrease cell growth through cell cycle arrest and cell death modulated by $\sigma_1$ and $\sigma_2$ receptors, respectively.

In agreement with other authors reporting that $\sigma_2$ agonists can modulate the expression of the mdr-1 gene through reverse transcription-PCR assay (26), we provided the first evidence that this class of drugs is directly able to reduce the amount of P-gp protein.

The consistent results obtained with PB28 as an anticancer agent and P-gp expression inhibitor suggested to combine this molecule with doxorubicin, which is conventionally used in breast cancer as a first-line antitumor drug. In fact, the P-gp overexpression is one of the main mechanisms specifically underlying the development of the doxorubicin-resistant phenotype often associated with recurrent breast cancer (28). The analysis of the cytotoxic efficacy of two sequential or simultaneous schedules highlighted that the two drugs together can act synergistically in a schedule-independent and cell line–independent manner. We hypothesize that the synergism could be due to enhanced apoptosis caused by doxorubicin and PB28 through two different pathways (i.e., caspase dependent and caspase independent, respectively; ref. 15). We further showed that this synergistic action was specifically P-gp mediated, performing similar experiments in presence or absence of verapamil, a specific P-gp functionality inhibitor. Finally, a PB28-dependent increase of intracellular accumulation of doxorubicin was shown. Even if the reduction of P-gp expression by PB28 is not specific for the anthracycline-resistant cell line, our findings support the hypothesis that this $\sigma_2$ agonist may enhance doxorubicin efficacy in drug-resistant tumors.
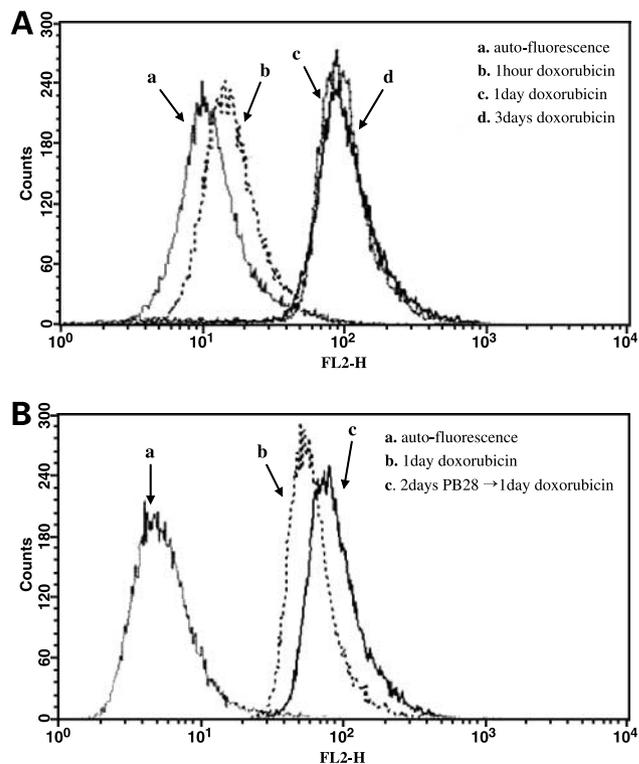
**Figure 5.** Intracellular doxorubicin accumulation in MCF7 ADR. Modulation of intracellular doxorubicin ($IC_{50}$) accumulation in MCF7 ADR as a function of time exposure and after pre-exposure with PB28. **A,** flow cytometry analysis of doxorubicin accumulation in MCF7 ADR cells after 1 h, 1 d, and 3 d of drug exposure. **B,** flow cytometry analysis of the ability of PB28 to enhance intracellular doxorubicin accumulation compared with doxorubicin alone when PB28 was given before doxorubicin.

**Table 3.** Doxorubicin intracellular accumulation

| Schedule | Intracellular doxorubicin amount (%)* | |
|---|---|---|
| | MCF7 | MCF7 ADR |
| Control | 0 | 0 |
| Doxorubicin 1 d | 100 | 100 |
| PB28 2 d then doxorubicin 1 d | $154 \pm 5$ | $175 \pm 6$ |
| | | |
| Control | 0 | 0 |
| Doxorubicin 1 d | 100 | 100 |
| PB28 1 d then PB28 and doxorubicin 1 d | $133 \pm 3.5$ | $150 \pm 5$ |

NOTE: Cells were treated with PB28 and/or doxorubicin and the cytotoxic drug was evaluated by flow cytometry. Percent drug accumulation with respect to the control 1-day doxorubicin alone (%).
*Mean ± SE of three independent experiments.

In conclusion, our results showed that our $\sigma_2$ agonist, PB28, inhibited cell growth, induced cell death through the modulation of $\sigma_1$ and $\sigma_2$ receptors, decreased P-gp expression, was able to cause a cytotoxically useful intracellular doxorubicin accumulation, and induced a caspase-independent apoptosis. If further *in vivo* experiments will confirm the results of our *in vitro* study, PB28 could really represent a novel pharmacologic strategy to increase the efficacy of conventional chemotherapy and to enhance P-gp-mediated chemosensitivity of some drug-resistant tumors.

**References**

**1.** Martin WR, Eades CE, Thompson JA, Huppler RE, Gilbert PE. The effects of morphine- and nalorphine-like drugs in the nondependent and morphine-dependent chronic spinal dog. J Pharmacol Exp Ther 1976;197: 517 – 32.

**2.** Su TP. Delineating biochemical and functional properties of $\sigma$ receptors: emerging concepts. Crit Rev Neurobiol 1993;7:187 – 203.

**3.** Walker JM, Hohmann AG, Hemstreet MK, et al. Functional role of $\sigma$ receptors in nervous system. In: Stone TW, editor. Aspect of synaptic transmission. Washington (DC): Taylor and Francis; 1993. p. 91 – 112.

**4.** Bowen WD. $\sigma$ Receptors: recent advances and new clinical potentials. Pharm Acta Helv 2000;74:211 – 8.

**5.** Langa F, Codony X, Tovar V, et al. Generation and phenotypic analysis of $\sigma$ receptor type I ($\sigma_1$) knockout mice. Eur J Neurosci 2003; 18:2188 – 96.

**6.** Aydar E, Palmer C, Klachko V, Jackson M. $\sigma$ Receptor as a ligand-modulated auxiliary potassium channel subunit. Neuron 2002;34: 399 – 410.

**7.** Hayashi T, Su TP. $\sigma$-1 receptors ($\sigma(1)$ binding sites) from raft-like microdomains and target lipid droplets on the endoplasmic reticulum: roles in endoplasmic reticulum lipid compartmentalization and export. J Pharmacol Exp Ther 2003;306:718 – 25.

**8.** Hayashi T, Maurice T, Su TP. Ca(2+) signaling via $\sigma(1)$-receptors: novel regulatory mechanism affecting intracellular Ca(2+) concentration. J Pharmacol Exp Ther 2000;293:788 – 98.

**9.** Alonso G, Phan V, Guillemain I, et al. Immunocytochemical localization of the $\sigma(1)$ receptor in the adult rat central nervous system. Neuroscience 2000;97:155 – 70.

**10.** Hanner M, Moebius FF, Flandorfer A, Knaus H-G, Striessnig J. Expression of the mammalian $\sigma$-1 binding site. Proc Natl Acad Sci U S A 1996;93:8072 – 7.

**11.** Hellewell SB, Bruce A, Feinstein G, Orringer J, Williams W, Bowen WD. Rat liver and kidney contain high densities if $\sigma$-1 and $\sigma$-2 receptors: characterization by ligand binding and photoaffinity labelling. Eur J Pharmacol Mol Pharmacol Sect 1994;268:9 – 18.

**12.** Monnet FP, Debonnel G, de Montigny C. *In vivo* electrophysiological evidence for a selective modulation of *N*-methyl-ᴅ-aspartate-induced neuronal activation in rat CA3 dorsal hippocampus by $\sigma$ ligands. J Pharmacol Exp Ther 1992;261:123 – 30.

**13.** Gonzalez-Alvear GM, Werling LL. $\sigma$ Receptor regulation of norepinephrine release from rat hippocampal slices. Brain Res 1995;673:61 – 9.

**14.** Monnet FP, de Costa BR, Bowen WD. Differentiation of $\sigma$ ligand-activated receptor subtypes that modulate NMDA-evoked [$^3$H]noradrenanaline release in rat hippocampal slices. Br J Pharmacol 1996;119:65 – 72.

**15.** Crawford KW, Bowen WD. $\sigma$-2 Receptor agonists activate a novel apoptotic pathway and potentiate antineoplastic drugs in breast tumor cell lines. Cancer Res 2002;62:313 – 22.

**16.** John CS, Vilner BJ, Schwartz AM, Bowen WD. Characterization of $\sigma$ receptor binding sites in human biopsied solid breast tumor. J Nucl Med 1996;37:267P.

**17.** Vilner BJ, John CS, Bowen WD. $\sigma$-1 and $\sigma$-2 Receptors are expressed in a wide variety of human and rodent tumor cell lines. Cancer Res 1995; 55:408 – 13.

**18.** Wheeler KT, Wang LM, Wallen CA, et al. $\sigma$-2 Receptors as a biomarker of proliferation in solid tumors. Br J Cancer 2000;82:1223 – 32.

**19.** Rowland DJ, Tu Z, Mach RH, Welch MJ. Investigation of a new $\sigma_2$ receptor ligand for detection of breast cancer. J Labelled Compd Radiopharm 2003;46:S1 – 403.

**20.** Brent PJ, Pang GT. $\sigma$ Binding site ligands inhibit cell proliferation in mammary and colon carcinoma cell lines and melanoma cells in culture. Eur J Pharmacol 1995;278:151 – 60.

**21.** Vilner BJ, de Costa BR, Bowen WD. Cytotoxic effects of $\sigma$ ligands: $\sigma$ receptor-mediated alterations in cellular morphology and viability. J Neurosci 1995;15:117 – 34.

**22.** Brent PJ, Pang G, Little G, Dosen PJ, Van Helden DF. The $\sigma$ receptor ligand, reduced haloperidol, induces apoptosis and increases intracellular-free calcium levels [Ca$^{2+}$] in colon and mammary adenocarcinoma cells. Biochem Biophys Res Commun 1996;219:219 – 26.

**23.** Crawford KW, Coop A, Bowen WD. $\sigma(2)$ Receptors regulate changes in sphingolipid levels in breast tumor cells. Eur J Pharmacol 2002;443: 207 – 9.

**24.** Vilner BJ, Bowen WD. Modulation of cellular calcium by $\sigma$-2 receptors: release from intracellular stores in human SK-N-SH neuroblastoma cells. J Pharmacol Exp Ther 2000;292:900 – 11.

**25.** Kawamura K, Kobayashi T, Matsuno K, Ishiwata K. Different brain kinetics of two $\sigma_1$ receptor ligands, [$^3$H](+)-pentazocine and [$^{11}$C]SA4503, by P-glycoprotein modulation. Synapse 2003;48:80 – 6.

**26.** Bowen WD, Jin B, Blann E, Vilner BJ, Lyn-Cook BD. $\sigma$ Receptor ligands modulate expression of the multi-drug resistance gene in human and rodent brain tumor cell lines. Proc Am Assoc Cancer Res 1997; 38:479.

**27.** Lehne G. P-glycoprotein as a drug target in the treatment of multidrug resistant cancer. Curr Drug Targets 2000;1:85 – 99.

**28.** Hait WN, Yang JM. Clinical management of recurrent breast cancer: development of multidrug resistance (MDR) and strategies to circumvent it. Semin Oncol 2005;32:S16 – 21.

**29.** Dumontet C, Sikic BI. Mechanisms of action of and resistance to antitubulin agents: microtubule dynamics, drug transport, and cell death. J Clin Oncol 1999;17:1061 – 70.

**30.** Ozvegy-Laczka C, Hegedus T, Varady G, et al. High-affinity interaction of tyrosine kinase inhibitors with the ABCG2 multidrug transporter. Mol Pharmacol 2004;65:1485 – 95.

**31.** Pusztai L, Wagner P, Ibrahim N, et al. Phase II study of tariquidar, a selective P-glycoprotein inhibitor, in patients with chemotherapy-resistant, advanced breast carcinoma. Cancer 2005;104:682 – 91.

**32.** Berardi F, Ferorelli S, Colabufo NA, Contino M, Perrone R, Tortorella V. 4-(Tetralin-1-yl- and naphthalen-1-yl)alkyl derivatives of 1-cyclohexylpiperazine as $\sigma$ receptor ligands with agonist $\sigma_2$ activity. J Med Chem 2004;47:2308 – 17.

**33.** Colabufo NA, Berardi F, Contino M, Perrone R, Tortorella V. A new method for evaluating $\sigma_2$ ligand activity in the isolated guinea-pig bladder. Naunyn Schmiedebergs Arch Pharmacol 2003;368:106–12.

**34.** Colabufo NA, Berardi F, Contino M, et al. Antiproliferative and cytotoxic effects of some $\sigma_2$ agonists and $\sigma_1$ antagonists in tumour cell lines. Naunyn Schmiedebergs Arch Pharmacol 2004;370:106–13.

**35.** Berardi F, Colabufo NA, Giudice G, et al. New $\sigma$ and 5-HT$_{1A}$ receptor ligands: $\omega$-(tetralin-1-yl)-*n*-alkylamine derivatives. J Med Chem 1996;39:176–82.

**36.** Chou TC, Talalay P. The median-effect principle and the combination index for quantification of synergism and antagonism. In synergism and antagonism in chemotherapy. In: Chou TC, Rideout DC, editors. San Diego: Academic Press; 1991. p. 61–102.

**37.** Taub ME, Podila L, Ely D, Almeida I. Functional assessment of multiple P-glycoprotein (P-gp) probe substrates: influence of cell line and modulator concentration on P-gp activity. Drug Metab Dispos 2005;33:1679–87.

**38.** Li J, Xu LZ, He KL, et al. Reversal effects of nomegestrol acetate on multidrug resistance in Adriamycin-resistant MCF7 breast cancer cell line. Breast Cancer Res 2001;3:253–63.

**39.** Yamamoto M, Torigoe T, Kamiguchi K, et al. A novel isoform of TUCAN is overexpressed in human cancer tissues and suppresses both caspase-8- and caspase-9-mediated apoptosis. Cancer Res 2005;65:8706–14.

**40.** Cheng YC, Prusoff WH. Relationship between the inhibition constant ($K_i$) and the concentration of inhibitor which causes 50 percent inhibition ($I_{50}$) of an enzymatic reaction. Biochem Pharmacol 1973;22:3099–108.

**41.** Vermes I, Haanen C, Steffens-Nakken H, Reutlingsperger C. A novel assay for apoptosis. Flow cytometric detection of phosphatidylserine expression on early apoptotic cells using fluorescein labelled Annexin V. J Immunol Methods 1995;184:39–51.

**42.** Gariboldi MB, Ravizza R, Riganti L, et al. Molecular determinants of intrinsic resistance to doxorubicin in human cancer cell lines. Int J Oncol 2003;22:1057–64.

**43.** Li D, Au JLS. Mdr1 transfection causes enhanced apoptosis by paclitaxel: an effect independent of drug efflux function of P-glycoprotein. Pharm Res 2001;18:907–13.

**44.** Vredenburg MR, Ojima I, Veith J, et al. Effects of orally active taxanes on P-glycoprotein modulation and colon and breast carcinoma drug resistance. J Natl Cancer Inst 2001;93:1234–45.

**45.** Qi J, Yang CZ, Wang CY, Yang M, Wang JH. Function and mechanism of pyronaridine: a new inhibitor of P-glycoprotein-mediated multidrug resistance. Acta Pharmacol Sin 2002;23:544–50.

**46.** Bem WT, Thomas GE, Mamone JY, et al. Overexpression of $\sigma$ receptors in nonneural human tumors. Cancer Res 1991;51:6558–62.

**47.** John CS, Bowen WD, Saga T, et al. A malignant melanoma imaging agent: synthesis, characterization, *in vitro* binding and biodistribution of iodite-125-(2-piperidinylaminoethyl)4-iodobenzamide. J Nucl Med 1993;34:2169–75.

**48.** John CS, Bowen WD, Fisher SJ, Lim BB, Vilner BJ, Wahl RL. Synthesis, *in vitro* pharmacologic characterization, and preclinical evaluation of *N*-[2-(1′-piperidinyl)ethyl]-3-[$^{125}$I]iodo-4-methoxybenzamide, P[$^{125}$I]MBA for imaging breast cancer. Nucl Med Biol 1999;91:105–14.

**49.** Renaudo A, Watry V, Chassot AA, Ponzio G, Ehrenfeld J, Soriani O. Inhibition of tumor cell proliferation by $\sigma$ ligand is associated with K$^+$ channel inhibition and p27$^{kip1}$ accumulation. J Pharmacol Exp Ther 2004;311:1105–14.